OPEN ACCESS Freely available online

PLoS GENETICS

Uncoupling Antisense-Mediated Silencing and DNA Methylation in the Imprinted *Gnas* Cluster

Christine M. Williamson[1], Simon T. Ball[1], Claire Dawson[2], Stuti Mehta[1], Colin V. Beechey[1], Martin Fray[3], Lydia Teboul[3], T. Neil Dear[3¤], Gavin Kelsey[2,4], Jo Peters[1]*

1 Medical Research Council Mammalian Genetics Unit, Harwell Science and Innovation Campus, Harwell, United Kingdom, **2** Laboratory of Developmental Genetics and Imprinting, The Babraham Institute, Cambridge, United Kingdom, **3** Medical Research Council Mary Lyon Centre, Harwell Science and Innovation Campus, Harwell, United Kingdom, **4** Centre for Trophoblast Research, University of Cambridge, Cambridge, United Kingdom

Abstract

There is increasing evidence that non-coding macroRNAs are major elements for silencing imprinted genes, but their mechanism of action is poorly understood. Within the imprinted *Gnas* cluster on mouse chromosome 2, *Nespas* is a paternally expressed macroRNA that arises from an imprinting control region and runs antisense to *Nesp*, a paternally repressed protein coding transcript. Here we report a knock-in mouse allele that behaves as a *Nespas* hypomorph. The hypomorph mediates down-regulation of *Nesp* in *cis* through chromatin modification at the *Nesp* promoter but in the absence of somatic DNA methylation. Notably there is reduced demethylation of H3K4me3, sufficient for down-regulation of *Nesp*, but insufficient for DNA methylation; in addition, there is depletion of the H3K36me3 mark permissive for DNA methylation. We propose an order of events for the regulation of a somatic imprint on the wild-type allele whereby *Nespas* modulates demethylation of H3K4me3 resulting in repression of *Nesp* followed by DNA methylation. This study demonstrates that a non-coding antisense transcript or its transcription is associated with silencing an overlapping protein-coding gene by a mechanism independent of DNA methylation. These results have broad implications for understanding the hierarchy of events in epigenetic silencing by macroRNAs.

Citation: Williamson CM, Ball ST, Dawson C, Mehta S, Beechey CV, et al. (2011) Uncoupling Antisense-Mediated Silencing and DNA Methylation in the Imprinted *Gnas* Cluster. PLoS Genet 7(3): e1001347. doi:10.1371/journal.pgen.1001347

Editor: Jeannie T. Lee, Massachusetts General Hospital, Howard Hughes Medical Institute, United States of America

Received July 20, 2010; **Accepted** February 18, 2011; **Published** March 24, 2011

Copyright: © 2011 Williamson et al. This is an open-access article distributed under the terms of the Creative Commons Attribution License, which permits unrestricted use, distribution, and reproduction in any medium, provided the original author and source are credited.

Funding: This work was supported by the UK Medical Research Council and the Biotechnology and Biological Sciences Research Council. The funders had no role in study design, data collection and analysis, decision to publish, or preparation of the manuscript.

Competing Interests: The authors have declared that no competing interests exist.

* E-mail: j.peters@har.mrc.ac.uk

¤ Current address: Section of Experimental Therapeutics, Disease Genetics Group, Leeds Institute of Molecular Medicine, St. James's University Hospital, Leeds, United Kingdom

Introduction

Over recent years it has emerged that most of the mammalian transcriptome is non-coding [1]. Several long non-coding transcripts have been implicated in epigenetic gene regulation and play essential, but incompletely understood, roles in epigenetic gene silencing in X-inactivation and genomic imprinting in mammals. For the latter, more than 100 imprinted genes are known in the mouse and most occur in clusters [2]. Parental specific gene silencing throughout the clusters is brought about by imprinting control regions (ICRs). These are regions that are differentially methylated in gametogenesis and are active when unmethylated. ICRs for three clusters, the *Igf2r* cluster, the *Kcnq1* cluster and the *Gnas* cluster, contain promoters for macroRNAs that are exclusively expressed from the paternally derived chromosome and run antisense to a protein coding gene that is repressed by the active unmethylated ICR (for reviews, see [3,4]). Two of these macroRNA genes, *Airn* in the *Igf2r* cluster and *Kcnq1ot1* in the *Kcnq1* cluster, have been shown to be key elements in parental specific silencing of all protein coding genes in their respective clusters [5-7], although their mode of action is incompletely understood. However both are known to be associated with the acquisition of repressive histone marks and DNA methylation marks of some genes. It is not yet known if the third gene for a macroRNA, *Nespas* in the *Gnas* cluster has a functional role (Figure 1). It is likely that several other imprinted gene clusters may share this regulatory principle, but their ICRs have not been defined functionally.

The ICR for the *Gnas* cluster contains the *Nespas* promoter [8] and lies within an extensive differentially methylated region, the *Nespas-Gnasxl* DMR, that acquires methylation in the maternal germline [9]. This DMR also contains the promoter for a protein coding paternally expressed transcript *Gnasxl*. The *Gnas* cluster, unusually, has a second maternally methylated germline DMR, the *Exon1A* DMR [10] that specifically controls maternal expression of transcripts arising from the *Gnas* promoter [11,12]. The ICR regulates the *Exon1A* DMR that in turn regulates the imprinted expression of *Gnas*. There is a third DMR in the *Gnas* cluster and this is a somatic DMR that becomes methylated on the paternal allele post-fertilisation [9,10]. This DMR covers the furthest upstream promoter in the cluster, the *Nesp* promoter. *Nesp* is maternally expressed, protein coding and is transcribed for about 80 kb through the whole cluster including the *Nespas-Gnasxl* DMR and the second germline DMR at *Exon1A*. Recently it was shown that truncation of this long *Nesp* transcript upstream of the two germline DMRs disrupted the acquisition of methylation at both DMRs in the oocyte [13]. Thus transcription of the *Nesp* protein coding transcript in the female germline is required for the

Author Summary

Genomic imprinting is a process resulting in expression of genes according to parental origin. Some imprinted genes are expressed when paternally derived and others when maternally derived. Thus imprinted genes are monoallelically expressed and one copy has to be silenced. There is evidence that some long non-coding RNAs, acting in *cis*, have a role in silencing. We investigated the role of *Nespas*, a gene for a non-coding RNA that is only expressed from the paternally derived chromosome in the *Gnas* cluster and runs antisense to its sense counterpart, *Nesp*. Expression of *Nespas* is associated with silencing of *Nesp* and a repressive methylation mark on the *Nesp* DNA. We generated a *Nespas* mutant with reduced levels of activity and showed that it down-regulated its sense counterpart *Nesp,* in the absence of a DNA methylation mark, but in the presence of an altered chromatin mark. We conclude that *Nespas* can repress *Nesp* by a mechanism independent of DNA methylation, by modulating a chromatin mark.

establishment of maternal methylation across the whole *Nespas-Gnasxl* DMR including the ICR as well as the *Exon1A* DMR.

The *Nesp* transcript is the sense counterpart of the paternally expressed antisense *Nespas*. The macroRNA *Nespas* that arises from a promoter within the ICR transcribes through, and is associated with methylation of the *Nesp* DMR [8], but the mechanisms for induction of the post-fertilisation methylation of the *Nesp* DMR on the paternal allele or, for that matter, any somatic DMR, have not been established. *De novo* establishment of methylation at maternal and some paternal germline DMRs requires the DNA methyltransferase DNMT3A and its non-enzymatic cofactor DNMT3L [14-16]. The process of methylation is mediated by histone modifications; it appears that DNMT3A is recruited to the DNA by complexing with DNMT3L [17-19] which interacts with histone H3 but only when lysine 4 is unmethylated [17]. Interaction of DNMT3A with chromatin is also inhibited by H3K4 methylation [20] but promoted by H3K36 trimethylation [21]. Whether *de novo* DNA methylation of somatic DMRs depends upon DNMT3A, or the second *de novo* enzyme DNMT3B, and co-operation with DNMT3L has not been established.

In order to investigate a role for *Nespas,* we made use of a knock-in allele that behaved as a *Nespas* hypomorph. We show here that when *Nespas* is present at a low level in the hypomorph the *Nesp* promoter is unmethylated but *Nesp* expression is considerably down-regulated and the *Nesp* promoter is only partially enriched for an activating histone mark, methylated H3K4. Thus, in the hypomorph, *Nespas* can mediate the down-regulation of *Nesp* through chromatin modification even in the absence of DNA methylation at *Nesp*. An insufficiency of methylated H3K4 could be a major factor in repressing *Nesp* expression. Furthermore, the results suggest that *Nespas* has a role in the demethylation of H3K4me3 as a prerequisite for DNA methylation of the *Nesp* promoter on the paternal chromosome. The results provide the first evidence that *Nespas* has a functional role in regulating imprinted gene expression in the *Gnas* cluster.

Results

Gene targeting generates a *Nespas* hypomorph (*Nesp-T^{int2}*)

In studies to analyse the regulatory function of *Nespas*, we made use of a *Nespas* hypomorph (*Nesp-T^{int2}*; phenotypic analysis to be

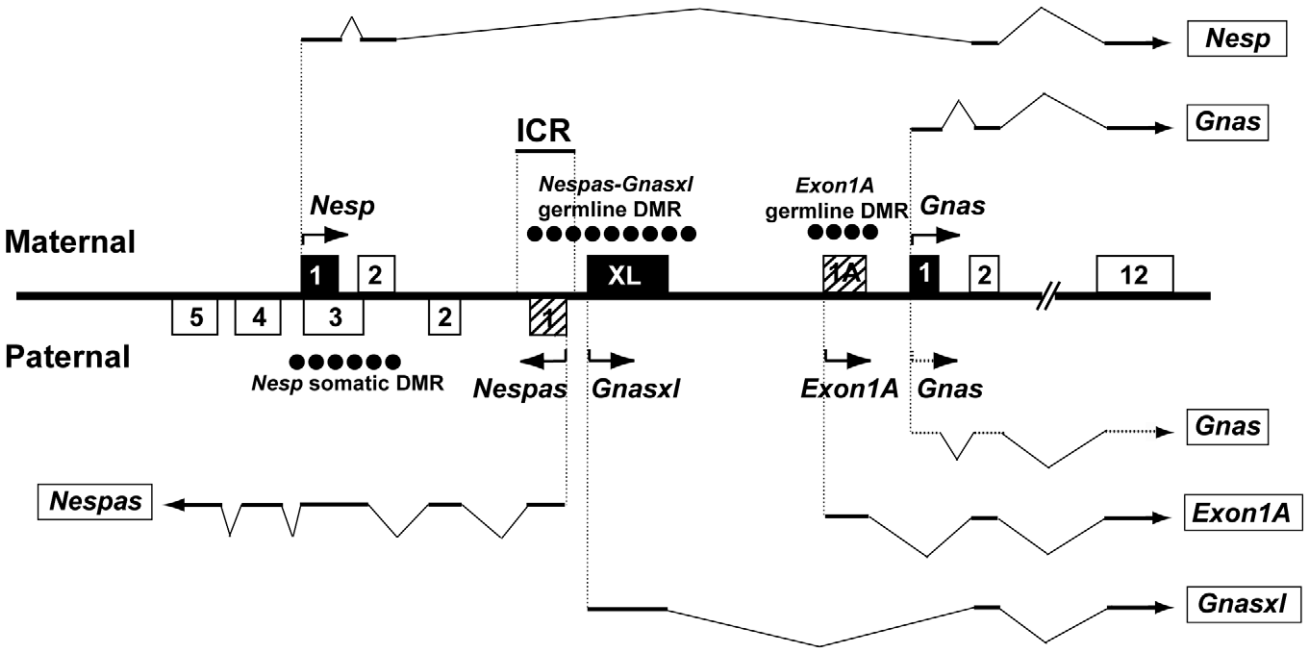

Figure 1. Overview of the mouse *Gnas* locus showing the organisation of the protein-coding transcripts *Nesp, Gnasxl*, and *Gnas* and the paternally expressed non-coding transcripts *Nespas* and *Exon1A*. Transcripts expressed from the maternally inherited allele are shown above the line, those from the paternally inherited allele are below the line and the direction of transcription is shown by arrow heads. Unspliced *Nespas* is not shown. The black filled boxes represent first exons of the protein-coding transcripts and the hashed filled boxes are the first exons of the non-coding transcripts. The first exons of *Nesp*, *Gnasxl, Exon1A* and *Gnas* all splice into exon 2 of *Gnas.* In a subset of tissues, *Gnas* itself is tissue-specifically imprinted; the dotted line shows the limited expression of *Gnas* from the paternal allele. The position of the differentially methylated regions (DMRs) are shown by rows of filled circles on the methylated allele; ICR, shows the position of the Imprinting Control Region [8]. Adapted from Peters and Williamson [49].
doi:10.1371/journal.pgen.1001347.g001

reported elsewhere). The hypomorph resulted from insertion of a polyadenylation cassette from the rabbit β-globin gene, into exon 1 of *Nespas*, in the reverse orientation (pA) so that truncation of *Nespas* should not occur (Figure 2A and 2B). Although it was not anticipated that this insertion would influence expression of *Nespas*, the mutant was shown to be a hypomorph in three ways. Firstly, we used RT-PCR and primers (Figure 2C) that would amplify *Nespas* but not *Nesp*. Weak expression of a *Nespas* splice variant was found in brain from newborn mice with a paternally derived *Nesp-T^{int2}* allele (+/*Nesp-T^{int2}*, note that the maternal allele precedes the paternal allele in all genotypes shown here; Figure 2D). Mice carrying a paternal copy of the null *Nespas* allele, Δ*NAS-DMR*, in which the *Nespas* promoter and first exon are deleted [8], were included as a negative control (Figure 2D). Secondly, the hypomorph was verified by RNA blot analysis using a single stranded probe, shown in Figure 2C, that would detect spliced and unspliced *Nespas* transcripts. The *Nespas* transcripts, which are detected as a smear [22], were considerably reduced in 15.5 dpc embryos with the paternally inherited *Nesp-T^{int2}* allele when compared to the wild-type level (Figure 2E). Thirdly, we checked that the primary transcripts of *Nespas* were reduced in +/*Nesp-T^{int2}* newborn brain using a TaqMan real-time qPCR assay. The assay was designed upstream of the *Nesp* promoter in intron 4 of *Nespas* [23] and is shown schematically in Figure 2C. We showed that *Nespas* levels were reduced by 94% in heterozygotes, +/*Nesp-T^{int2}*, that have a paternally inherited copy of the mutation when compared to wild-type levels ($P = 5.91 \times 10^{-11}$; Figure 2F). The reduced level of *Nespas* was not due to gain of methylation on the paternal allele at the *Nespas-Gnasxl* DMR (Figure S1). Thus the position of the cassette close to the *Nespas* promoter may have affected promoter activity, resulting in a low level of *Nespas*.

Paternal inheritance of *Nesp-T^{int2}* is associated with hypomethylation of the paternal *Nesp* somatic DMR and partial de-repression of *Nesp*

Previous work had shown paternal inheritance of the null Δ*NAS-DMR* allele was associated with loss of methylation of the *Nesp* promoter [8]. Therefore we investigated whether a low level of *Nespas* from the paternal allele in +/*Nesp-T^{int2}* was associated with a change in the methylation status of the *Nesp* somatic DMR. Southern analysis of newborn liver showed complete loss of methylation at the *Nesp* promoter and first exon on the paternal allele in **+/***Nesp-T^{int2}* (Figure 3A, Top Right). This result was confirmed by bisulphite analysis of brain DNA from newborn offspring arising from crosses of *Nesp-T^{int2}* carrier males with SD2 females carrying the *Gnas* cluster region from *Mus spretus*. The presence of single nucleotide variants in the parents enabled the distinction of maternal and paternal *Nesp* alleles. Two wild-type (+^{SD2}/+) and four mutant (+^{SD2}/*Nesp-T^{int2}*) newborns were analysed and Figure 3A (Bottom Right) shows loss of methylation on the paternal allele of **+/***Nesp-T^{int2}* compared with that of a wild-type. Thus the normally methylated paternal *Nesp* allele was unmethylated in **+/***Nesp-T^{int2}*, probably due to the low level of *Nespas* (as summarised in Figure 3A, Left).

As the paternally derived *Nesp* DMR was unmethylated in +/*Nesp-T^{int2}*, we expected that *Nesp* would be expressed from the mutant paternal allele. In addition, as *Nesp* and *Nespas* overlap (Figure 1), insertion of the polyadenylation cassette in exon 1 of *Nespas* on the antisense strand is also an insertion into intron 2 of *Nesp* on the sense strand and might truncate *Nesp*. Sequence analysis of RT-PCR products derived from using a *Nesp* exon 2-specific forward primer and a reverse primer specific to the polyadenylation cassette and therefore specific to the mutant paternal allele revealed a number of splice variants (Figure S2) whereby *Nesp* splices into the inserted β-globin sequence. Thus *Nesp* was expressed from the paternal allele and was likely to be truncated. The sizes of the *Nesp* transcripts in +/*Nesp-T^{int2}* embryos were analysed by northern blotting (Figure 3B). Two major transcripts were detected: full length *Nesp* transcript as expected from the unaltered maternal allele and a smaller weaker band, consistent with *Nesp*, from the targeted paternal allele, being spliced and truncated in the second intron of *Nesp*.

Quantification of the *Nesp* level in +/*Nesp-T^{int2}* newborn brain by real time RT-qPCR was undertaken using a TaqMan assay in which the probe spanned the junction of exon 1 and 2 of *Nesp* (Table S1). This showed the level of *Nesp* transcript was elevated to some extent in +/*Nesp-T^{int2}* but was not double the wild-type level expected for full biallelic expression (Figure 3B). The quantification was consistent with full expression from the maternal allele and diminished expression from the mutant paternal allele.

To check whether the insertion of the polyadenylation cassette had disrupted a genomic sequence necessary for full expression of *Nesp*, we analysed the level of *Nesp* when the polyadenylation cassette was inserted at the same site in *Nespas* exon 1 but in the opposite orientation (allele *Nespas-T^{ex1}*; Figure 4A and 4B; phenotypic analysis to be reported elsewhere). On paternal inheritance insertion of the cassette caused, as expected, truncation of *Nespas* (Figure 4C and Figure S3A). Furthermore there was loss of methylation at the *Nesp* DMR on the paternal allele in +/*Nespas-T^{ex1}* (Figure 4D). This was consistent with complete loss of silencing of *Nesp* from the paternal allele (Figure 4E). The *Nesp* level was increased as shown by northern blotting and confirmed to be double dose when quantified using a TaqMan assay for measuring *Nesp* exon 1 spliced onto exon 2. The increase in *Nesp* expression was from the normally silent paternal allele (Figure S3B). As full expression of *Nesp* was detected from the paternal allele when the genomic sequence was disrupted in +/*Nespas-T^{ex1}*, it was unlikely that the reduced level of *Nesp* from the paternal allele in +/*Nesp-T^{int2}* was due to the disruption of a DNA element. However, it could be due to reduced stability of the *Nesp* transcripts from the *Nesp-T^{int2}* allele and/or regulation of *Nesp* by *Nespas*.

Expression of *Nespas* on the maternal allele in *Nesp-T^{int2}*/+

It was known that on the wild-type maternal allele, *Nesp* is expressed and the extensive *Nespas-Gnasxl* DMR that contains the ICR for the cluster is methylated. Recently the mutant allele *Nesp^{trun}*, which leads to truncation of the *Nesp* transcript at *Nesp* exon 2, was shown to be associated with variable, germline-derived loss of methylation of the *Nespas-Gnasxl* DMR on the maternal allele [13]. Thus some carriers lost methylation of the *Nespas-Gnasxl* DMR but others did not. It is expected that in those that have lost methylation *Nespas* is expressed, but in those that retain methylation *Nespas* is repressed. If a similar variation in the methylation of the *Nespas-Gnasxl* DMR and *Nespas* expression occurred on maternal inheritance of *Nesp-T^{int2}* where *Nesp* is truncated (Figure 5A) in intron 2, much further 3′ than in *Nesp^{trun}* then we could test whether maternal inheritance of the *Nesp-T^{int2}* allele has a similar effect to maternal transmission of *Nesp^{trun}* on methylation of the *Nespas* DMR.

Firstly, *Nesp-T^{int2}*/+^{129} heterozygotes in which the wild-type paternal allele was derived from 129/SvEv were used. Variable loss of methylation at the *Nespas-Gnasxl* DMR region was found by Southern (Figure 5B). Some *Nesp-T^{int2}*/+^{129} animals had lost methylation on the mutant maternal allele and in other animals within the same litter, the allele remained methylated. Secondly, *Nesp-T^{int2}*/+^{SD2} heterozygotes, in which the paternal allele was derived from SD2 to enable the parental origin to be distinguished

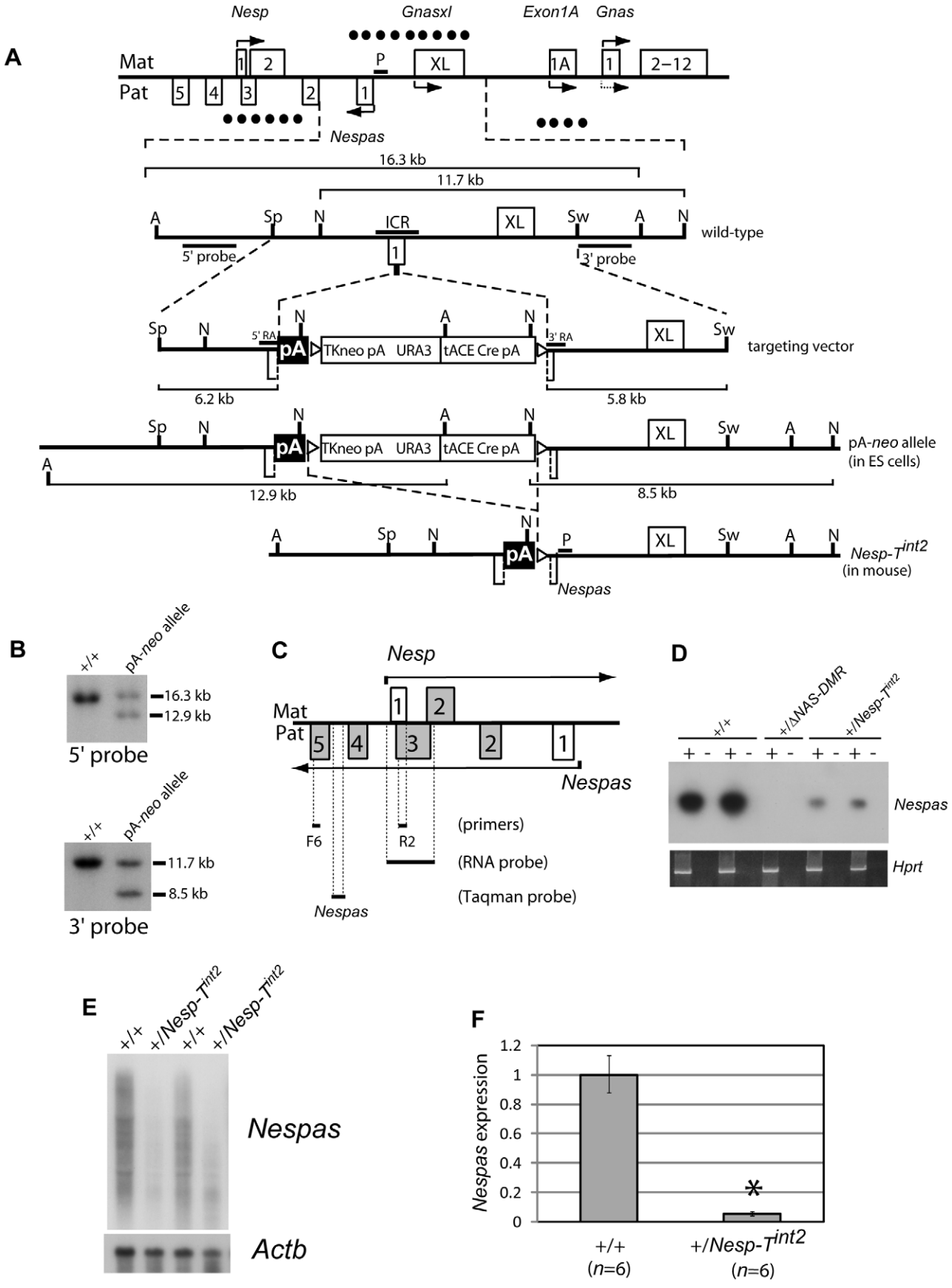
A
Nesp
Gnasxl
Exon1A
Gnas
Mat
Pat
Nespas
16.3 kb
11.7 kb
wild-type
5' probe
3' probe
ICR
XL
targeting vector
TKneo pA
URA3
tACE Cre pA
6.2 kb
5.8 kb
pA-neo allele
(in ES cells)
12.9 kb
8.5 kb
Nesp-T int2
(in mouse)
B
+/+
pA-neo allele
16.3 kb
12.9 kb
5' probe
11.7 kb
8.5 kb
3' probe
C
Nesp
Nespas
(primers)
F6
R2
(RNA probe)
(Taqman probe)
D
+/+
+/ΔNAS-DMR
+/Nesp-T int2
Nespas
Hprt
E
+/+
+/Nesp-T int2
Nespas
Actb
F
Nespas expression
1.2
1
0.8
0.6
0.4
0.2
0
+/+
(n=6)
+/Nesp-T int2
(n=6)

Figure 2. The targeted allele, *Nesp-T^{int2}*, is a *Nespas* hypomorph when paternally inherited. (A) Overview of the mouse *Gnas* locus showing enlargement of the *Nespas* region and the site of insertion of the rabbit β-globin polyadenylation cassette in *Nespas* exon 1. The targeting vector shows the location of a 1.2 kb fragment (pA) from the rabbit β-globin gene to truncate *Nesp*, and the selection genes were flanked by *loxP* sites (open triangles). The selection genes were deleted from the pA-*neo* targeted allele upon male germline transmission by Cre-recombinase mediated excision to generate *Nesp-T^{int2}*. The DMRs are shown by the presence of filled circles on the methylated allele. A, *Avr*II; N, *Nde*I; Sp, *Spe*I; Sw, *Swa*I; P, *Nespas* promoter; ICR, Imprinting Control Region, the extent of which is defined by the deletion in the Δ*NAS-DMR* allele [8]. (B) Southern analysis of ES cell DNA from wild-type (+/+) and targeted (pA-*neo*) cells. The pA-*neo* targeted clones were identified by the presence of an 8.5 kb *Nde*I fragment detected with the 3′ external probe. Correct targeting at the 5′ end was confirmed by the detection of a 12.9 kb *Avr*II fragment with the 5′ external probe. (C) Schematic of the *Nesp-Nespas* region showing overlapping transcription on the sense and antisense strands and the position of RT-PCR primers, a single stranded RNA probe and TaqMan assay for detecting the primary *Nespas* transcript. (D) RT-PCR analysis of *Nespas* in neonatal brain after paternal transmission of *Nesp-T^{int2}* (+/*Nesp-T^{int2}*) using primers F6 and R2 (Figure 2C; Table S1). +/Δ*NAS-DMR*, mice with paternal deletion of the ICR [8]; + and −, presence and absence of reverse transcriptase, respectively; *Hprt*, amplification control. (E) RNA blot analysis showing expression of *Nespas* in poly(A)$^+$ RNA from 15.5 dpc embryos using the single stranded RNA probe shown in Figure 2C. (F) Bar chart showing the relative level of *Nespas* expression in newborn brain by RT-qPCR using a TaqMan assay within intron 4 (Figure 2C). The reference gene was *Gapdh*. Error bars (RQmin/RQmax) were based on a 95% confidence level.
doi:10.1371/journal.pgen.1001347.g002

using single nucleotide variants, were used. Southern analysis of twelve *Nesp-T^{int2}*/+^{SD2} newborns from two litters showed no loss of methylation in five (42%; designated *Nesp-T^{int2}*/+ (methylated)) and loss of methylation in seven (58%). Further investigation of the latter class by bisulphite analysis was carried out. Bisulphite sequence profiles of the seven newborns with loss of methylation confirmed the *Nespas* promoter region was completely unmethylated on the mutant maternal allele in six (designated *Nesp-T^{int2}*/+ (unmethylated)), and partially methylated in one (data not shown). Thus variable loss of methylation of the *Nespas-Gnasxl* DMR occurs on maternal inheritance of *Nesp-T^{int2}* just as it does with *Nesp^{trun}*.

We predicted that *Nespas* would be silent in the *Nesp-T^{int2}*/+ (methylated) mice, but expressed in the *Nesp-T^{int2}*/+ (unmethylated) mice. To check that the detectable level of *Nespas* was low from the mutant *Nesp-T^{int2}* allele on maternal inheritance as it is on paternal inheritance, we used RT-PCR and double heterozygotes, *Nesp-T^{int2}*/Δ*NAS-DMR* (Figure 5C) that had a maternal copy of *Nesp-T^{int2}* and a paternal copy of the *Nespas* promoter deletion allele, Δ*NAS-DMR* [8]. As *Nespas* is not expressed from the Δ*NAS-DMR* allele (Figure 5D), any expression of *Nespas* in the double heterozygotes must be from the mutant maternal allele, *Nesp-T^{int2}*. As expected, a low level of *Nespas* was detected in three double heterozygotes, within one litter (Figure 5D), showing that *Nespas* is expressed from the maternal allele and that the *Nesp-T^{int2}* allele is a hypomorph on maternal inheritance as well as on paternal inheritance. Bisulphite sequence analysis of one of the three double heterozygotes confirmed the active *Nespas* allele was unmethylated (Figure S4). *Nespas* expression was not detected in a fourth double heterozygote (Figure 5D) and bisulphite sequencing showed the inactive allele was methylated (Figure S4).

Maternal inheritance of *Nesp-T^{int2}* is associated with down-regulation of *Nesp*

The finding that maternal inheritance of *Nesp-T^{int2}* resulted in two classes of offspring, one in which *Nespas* was repressed and one in which *Nespas* was expressed, enabled us to test whether *Nespas* expression was associated with down-regulation of *Nesp*. If the level of *Nesp* was lower in the *Nespas* expressing class than in the class in which *Nespas* was repressed this would provide evidence that *Nespas* regulates *Nesp* expression. Both classes carried identical *Nesp-T^{int2}* alleles on the maternally derived chromosome so any effects on the levels of *Nesp* transcript, such as stability, due to the sequence of the mutant allele should be the same in both classes. Using the TaqMan RT-qPCR assay that measures *Nesp* exon 1 spliced onto exon 2, a significant difference in *Nesp* level was detected between four *Nesp-T^{int2}*/+^{SD2} (methylated) and four *Nesp-T^{int2}*/+^{SD2} (unmethylated) littermates (Figure 5E; $P = 5.36\times10^{-3}$). The *Nesp* level was three-fold lower when the *Nespas* DMR was unmethylated and *Nespas* is transcribed compared to when the DMR was methylated. Similar results were obtained on a 129/SvEv background between *Nesp-T^{int2}*/+^{129} (methylated) and *Nesp-T^{int2}*/+^{129} (unmethylated) mice (data not shown).

The reduced level of *Nesp* in *Nesp-T^{int2}*/+^{SD2} (unmethylated) was not due to a small gain of methylation at the *Nesp* DMR on the maternal allele (Figure S5). Thus we have shown that expression of *Nespas*, even at a low level, was sufficient to down-regulate *Nesp* in the absence of DNA methylation, (summarised in Figure 5E) and provide the first evidence for *Nespas*-mediated silencing of *Nesp*.

Altered histone modifications at the *Nesp* DMR associated with *Nespas* transcription in *Nespas* knock-in mutants

Our interpretation from both maternal and paternal inheritance of the hypomorph *Nesp-T^{int2}* is that *Nespas* transcript/transcription is associated with down-regulation of *Nesp* expression in the absence of methylation of the *Nesp* DMR. We next tested whether there were histone modifications at *Nesp* that would account for its down-regulation on the paternal allele in +/*Nesp-T^{int2}*. We also tested +/*Nespas-T^{ex1}* in which *Nesp* is fully expressed on the paternal allele, and wild-type in which *Nesp* is silent. As *Nesp* and *Nespas* are expressed in mouse embryonic fibroblast cells (MEFs), we used chromatin prepared from MEFs of wild-type, +/*Nesp-T^{int2}* and +/*Nespas-T^{ex1}*, on a SD2 background, and analysed histone modifications, H3K4me3, H3K9me3, H3K27me3 and H3K36me3 at three regions (designated 1–3; Figure 6A). Region 1 was within a fragment previously shown to have promoter activity (data not shown), region 2 spanned the first intron and part of exon 2, and region 3 was just downstream of *Nesp* exon 2 in intron 2. Regions 1–3 were chosen as they had been shown to be associated with the activating mark, H3K4me3, and the repressive mark, H3K9me3 on the maternal and paternal allele of *Nesp*, respectively, in skin fibroblasts (designated Allelic ChIP sites 2, 3 and 4, respectively; [24]). Similarly, H3K4me3 and the repressive mark H3K27me3 were found associated with the 5′ end of *Nesp* in MEFs but allelic specificity was not analysed [25]. H3K36me3 was included as a marker for transcriptional elongation [26].

Consistent with the reports above, in wild-type MEFs there was depletion of the active mark H3K4me3 on the paternal allele in comparison to the maternal allele at all three regions analysed and enrichment of the repressive mark H3K9me3 at regions 1 and 3 (Figure 6B). Surprisingly, there was also depletion of H3K27me3 on the paternal allele relative to the maternal allele in wild-type MEFs. These results suggest that H3K9me3 constitutes the repressive mark at the *Nesp* promoter and DMR in these cells. H3K36me3 showed no parental-allele enrichment, which might

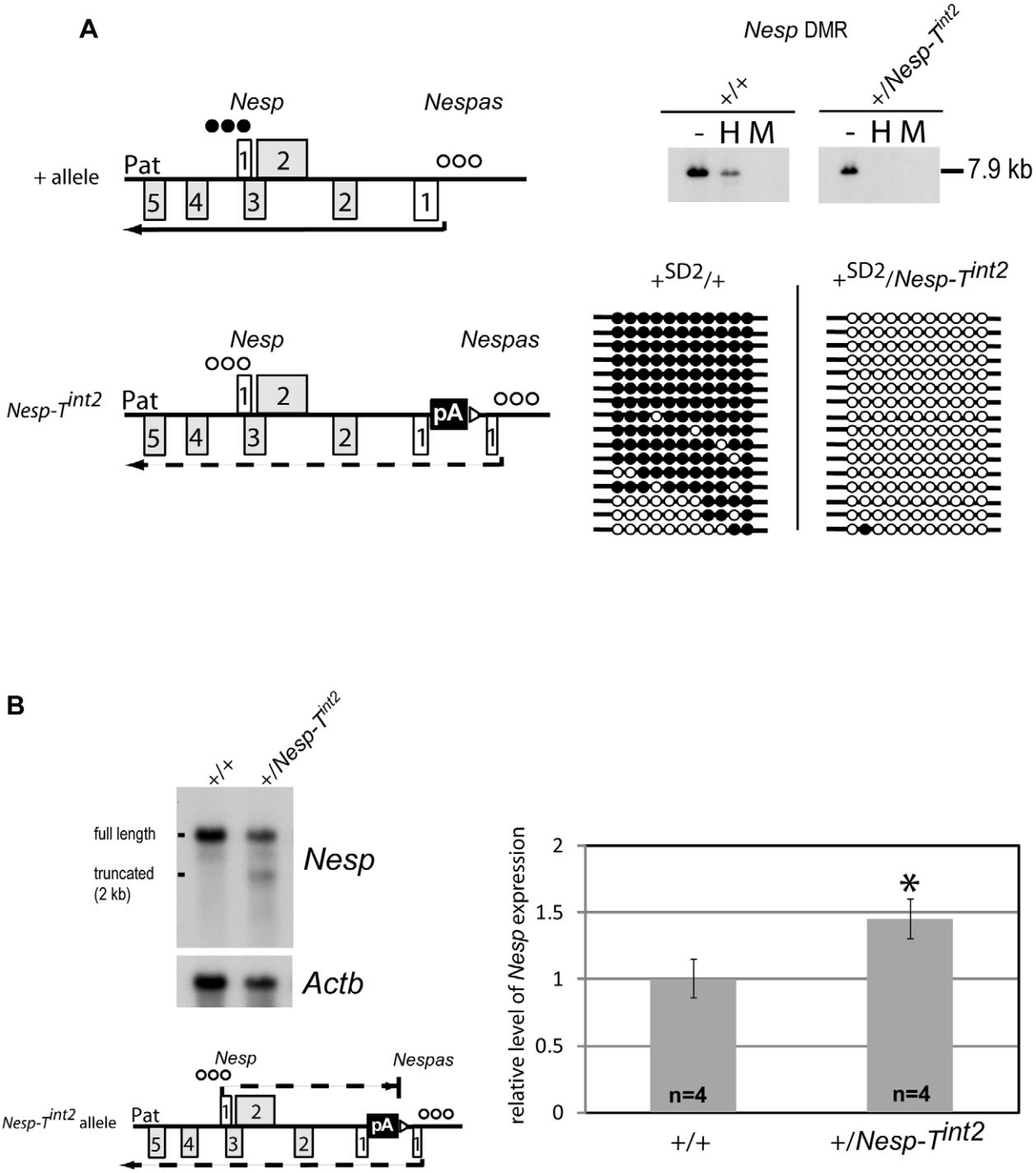

Figure 3. *Nesp* is expressed and truncated from the paternal allele in +/*Nesp-T*^{int2}. (A) Loss of methylation at the *Nesp* DMR in +/*Nesp-T*^{int2}. (A Left) Schematic summary of the transcriptional status of *Nespas* and the methylation status of *Nespas* and *Nesp* on the paternal allele of wild-type and +/*Nesp-T*^{int2}. Dashed line indicates low level of transcript. Row of filled circles, methylated allele; row of open circles, unmethylated allele. (A Top Right) Southern analysis showing promoter methylation at the *Nesp* DMR is lost in +/*Nesp-T*^{int2}. Genomic DNA from newborn liver was digested with *Eco*RI (-), *Eco*RI and *Hpa*II (H), or *Eco*RI and *Msp*I (M). (A Bottom Right) Bisulphite profile of the paternal allele of the *Nesp* DMR in newborn brain from +^{SD2}/+ and +^{SD2}/*Nesp-T*^{int2}. Sequence variants allowed the maternal and paternal alleles to be discriminated; see Table S1 for primers. Each row of circles represented a clone derived from the paternal allele and each circle corresponded to a separate CpG (filled circles, methylated CpGs; open circles, unmethylated CpGs). Each block of circles represented the data from an individual mouse. (B) Low level of truncated *Nesp* from the paternal allele in +/*Nesp-T*^{int2}. (B Top Left) RNA blot analysis showing expression of *Nesp* in poly(A)$^+$ RNA from 15.5 dpc embryos using the single stranded RNA probe shown in Figure 2C. The full length transcript was expressed from the maternal allele. (B Bottom Left)The smaller truncated transcript was expressed from the targeted paternal allele as summarised in the schematic. (B Right) Bar chart showing the relative level of *Nesp* expression in newborn brain by RT-qPCR, measured using a TaqMan assay that detects exon 1 spliced onto 2. The reference gene was *Gapdh*. Error bars (RQmin/RQmax) were based on a 95% confidence level.
doi:10.1371/journal.pgen.1001347.g003

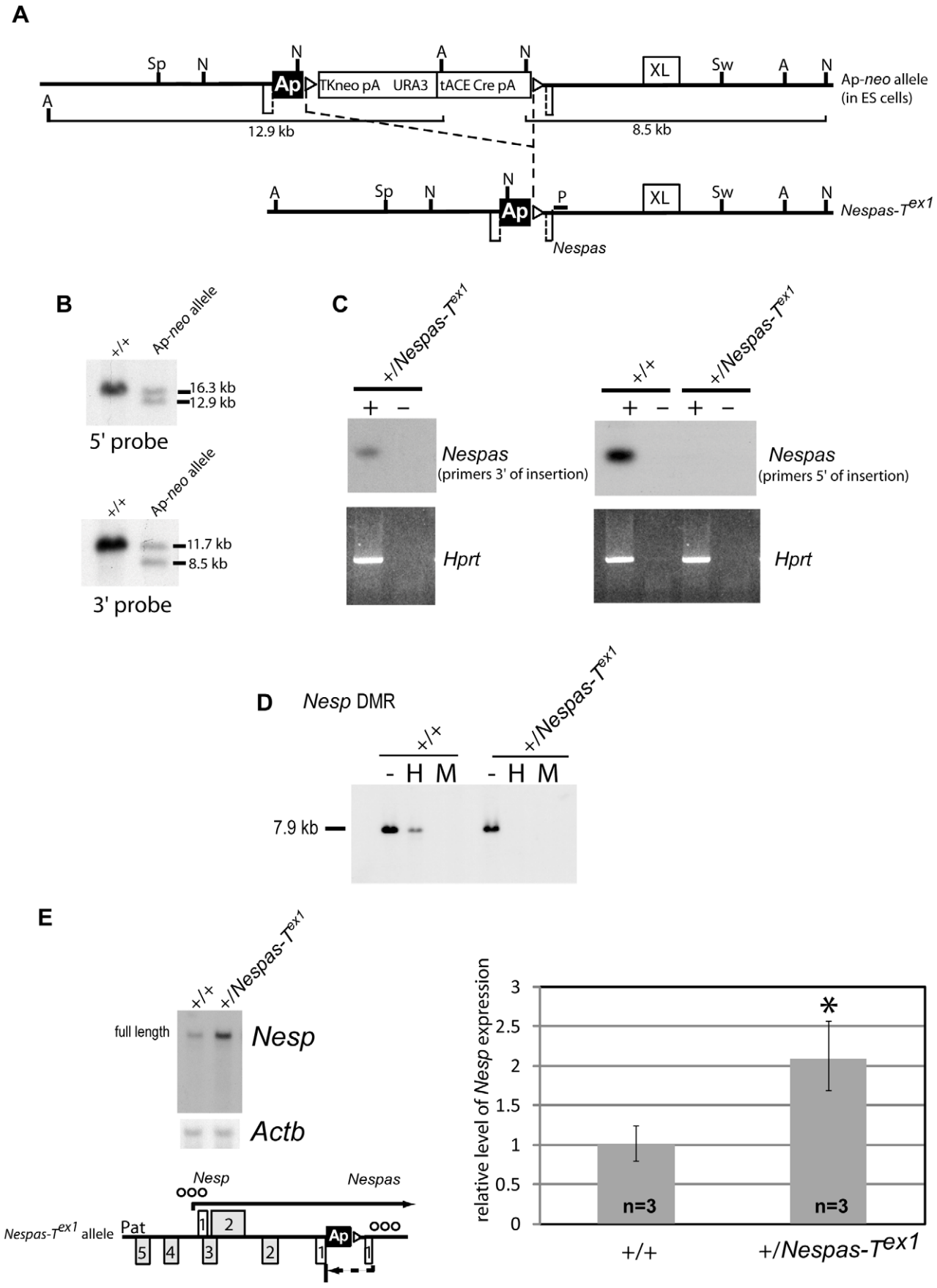
A
Sp
N
N
A
N
Ap
TKneo pA
URA3
tACE Cre pA
XL
Sw
A
N
Ap-neo allele
(in ES cells)
A
12.9 kb
8.5 kb
A
Sp
N
N
P
Ap
XL
Sw
A
N
Nespas-Tex1
Nespas
B
+/+
Ap-neo allele
16.3 kb
12.9 kb
5' probe
+/+
Ap-neo allele
11.7 kb
8.5 kb
3' probe
C
+/Nespas-Tex1
+ −
Nespas
(primers 3' of insertion)
Hprt
+/+
+/Nespas-Tex1
+ − + −
Nespas
(primers 5' of insertion)
Hprt
D
Nesp DMR
+/+
+/Nespas-Tex1
- H M - H M
7.9 kb
E
+/+
+/Nespas-Tex1
full length
Nesp
Actb
Nesp
Nespas
Nespas-Tex1 allele
Pat
1
2
5
4
3
2
1
Ap
1
relative level of Nesp expression
3
2.5
2
1.5
1
0.5
0
*
n=3
n=3
+/+
+/Nespas-Tex1

Figure 4. *Nesp* is fully expressed from the paternal allele in +/*Nespas-T*^{ex1}. (A) The *Nespas-T*^{ex1} allele was generated by targeting and is identical to *Nesp-T*^{int2} except that the polyadenylation cassette was inserted in the opposite orientation (Ap) to truncate *Nespas*. The selection genes were deleted from the Ap-*neo* targeted allele upon germline transmission by Cre-recombinase mediated excision to generate *Nespas-T*^{ex1}. (B) Southern analysis of ES cell DNA from wild-type (+/+) and targeted (Ap-*neo*) cells. The Ap-*neo* targeted clones were identified by the presence of an 8.5 kb *Nde*I fragment detected with the 3′ external probe. Correct targeting at the 5′ end was confirmed by the detection of a 12.9 kb *Avr*II fragment with the 5′ external probe. (C) RT-PCR assay in newborn brain showing *Nespas* is truncated. A primer pair, 3′ of the insertion, detected *Nespas* whereas a primer pair 5′ of the insertion did not detect *Nespas*. Symbols + and −, refer to reactions carried out in the presence and absence of reverse transcriptase, respectively. As the *Nespas* PCR products were weak, it was necessary to blot and probe the *Nespas* RT-PCR products with appropriate genomic probes. *Hprt* was included as an amplification control. (D) Southern analysis showing promoter methylation at the *Nesp* DMR is lost in +/*Nespas-T*^{ex1}. Genomic DNA from newborn brain was digested with *Eco*RI (-), *Eco*RI and *Hpa*II (H) or *Eco*RI and *Msp*I (M). (E) Biallelic expression of *Nesp* in +/*Nespas-T*^{ex1}. (E Top Left) RNA blot analysis showing expression of *Nesp* in poly(A)$^+$ RNA from 15.5 dpc embryos. (E Bottom Left) Schematic summary of the transcriptional and methylation status of *Nespas* and *Nesp* on the paternal allele of +/*Nespas-T*^{ex1}. (E Right) Bar chart showing the relative level of *Nesp* expression in newborn brain by RT-qPCR, measured using a TaqMan assay that detects exon 1 spliced onto 2. The reference gene was *Gapdh*. Error bars (RQmin/RQmax) were based on a 95% confidence level.
doi:10.1371/journal.pgen.1001347.g004

be consistent with the region being transcribed on both strands, corresponding to *Nesp* and *Nespas*, in wild-type MEFs.

The most striking finding in the mutants +/*Nesp-T*^{int2} and +/*Nespas-T*^{ex1} was that the depletion of H3K4me3 on the paternal allele seen in the wild-type MEFs was eliminated (Figure 6B). Furthermore, in the +/*Nespas-T*^{ex1} MEFs there was an even greater enrichment for H3K4me3 on the paternal allele at region 1 within the promoter region of *Nesp*. Thus truncation of *Nespas* and full expression of *Nesp* from the paternal allele in the *Nespas* truncation mutant +/*Nespas-T*^{ex1} was associated with a high level of H3K4me3 whereas low levels of *Nespas* and *Nesp* in the hypomorph +/*Nesp-T*^{int2} were associated with a lower level of H3K4me3. Our results suggest that *Nespas* transcript or transcription mediates the level of enrichment of the activating mark H3K4me3 in the absence of DNA methylation. Furthermore, an insufficiency of H3K4me3 is likely to be a major factor in depressing *Nesp* expression in the hypomorph.

There were also significant differences between wild-type, +/*Nesp-T*^{int2} and +/*Nespas-T*^{ex1} in the amount of H3K36me3 at region 1, and these correlate with *Nespas* transcription. Thus, in contrast to the equal allelic enrichment in wild-type MEFs, there was depletion of H3K36me3 on the paternal allele in +/*Nesp-T*^{int2} where there is a reduced level of *Nespas*, and further depletion of H3K36me3 in +/*Nespas-T*^{ex1} where *Nespas* is truncated and is not transcribed across the *Nesp* exons and promoter. The reduction in enrichment of H3K36me3 on the paternal allele is further evidence that transcription downstream of the inverted pA cassette is reduced on the *Nesp-T*^{int2} allele.

Differences in the allelic enrichment of the repressive marks H3K9me3 and H3K27me3 were also detected, but were less notable. For H3K9me3 it appeared that the relative enrichment on the paternal allele was reduced in MEFs from both mutants, but this reached significance only for region 3 in +/*Nespas-T*^{ex1}, and this accords with full expression of *Nesp* in +/*Nespas-T*^{ex1}. For H3K27me3, the depletion on the paternal allele observed in wild-type MEFs also tended to have been eroded, and this effect was significant at regions 2 and 3. Altered allelic enrichment of H3K27me3 was also detected in newborn brain in +/*Nespas-T*^{ex1} (data not shown). These results suggest that H3K27me3 is not normally a repressive mark on the wild-type paternal allele and that the increased amount in the mutants could be due to absence of DNA methylation, as previously observed at the imprinted *Rasgrf1* locus [27].

Effects on other transcripts in the *Gnas* cluster

Paternal inheritance of *Nesp-T*^{int2} resulted in weak expression both of *Nespas* and truncated *Nesp* so we next investigated whether there were additional effects on the other transcripts and DMRs in the *Gnas* cluster.

On paternal inheritance of *Nesp-T*^{int2}, levels of the normally paternally expressed *Gnasxl* transcript were reduced (Figure S6), but the reduction in expression was not due to gain of methylation at the *Gnasxl* promoter on the paternal allele (Figure S1). As the cassette was inserted close to the *Gnasxl* promoter, it is likely that the position of the insertion had affected the promoter activity of *Gnasxl* in some way.

On maternal inheritance of *Nesp-T*^{int2} where *Nesp* was truncated, there was invariable loss of methylation at the *Exon1A* DMR both when the *Nespas* DMR was methylated and when it was unmethylated (Figure S7). This result is similar to findings on maternal inheritance of *Nesp*^{trun} in which the *Nesp* transcript is truncated at its second exon [13], much further 5′ than in *Nesp-T*^{int2}.

As found with paternal inheritance of *Nesp-T*^{int2}, paternal inheritance of *Nespas-T*^{ex1} also led to reduced levels of *Gnasxl* (Figure S6) in the absence of methylation of the *Gnasxl* promoter (Figure S8), and was also attributable to the position of the inserted polyadenylation cassette.

On the maternal allele in *Nespas-T*^{ex1}/+ mice, full length *Nesp* remained expressed and *Gnasxl* and *Exon1A* remained repressed (Figure S9). In keeping with this, the *Nespas-Gnasxl* and *Exon1A* DMRs remained methylated on the maternal allele (Figure S10) thus showing that the altered methylation at the two germline DMRs in *Nesp-T*^{int2}/+ was not due to disruption of a DNA element by insertion of the cassette.

Discussion

Here we provide evidence that *Nespas*, a gene for a non-coding macroRNA has a role in imprinted gene silencing in the *Gnas* cluster. Furthermore we have shown that the *Nespas* transcript or its transcription has a role in setting the histone modifications permissive for DNA methylation of the DMR [17,20,21]. The functional evidence for these findings came from studies of *Nespas* mutants.

Nespas mediates imprinted gene silencing

Our finding that a low level of maternally expressed *Nespas* was sufficient to reduce *Nesp* levels is the first direct evidence for *Nespas*-mediated silencing of *Nesp*. This observation is consistent with partial de-repression of paternal *Nesp* in the *Nespas* hypomorph and complete loss of silencing of paternal *Nesp*, when paternal *Nespas* is either truncated or not expressed at all as in the ICR deletion ([8]; summarised in Figure 7).

From the current study, *Nespas* can be added to the small number of antisense non-coding genes that have been shown to have a functional role in gene silencing. These include *Tsix*, a negative regulator of the non-coding RNA, *Xist* (for review, see [28]) that is required for X-inactivation [29] as well as two

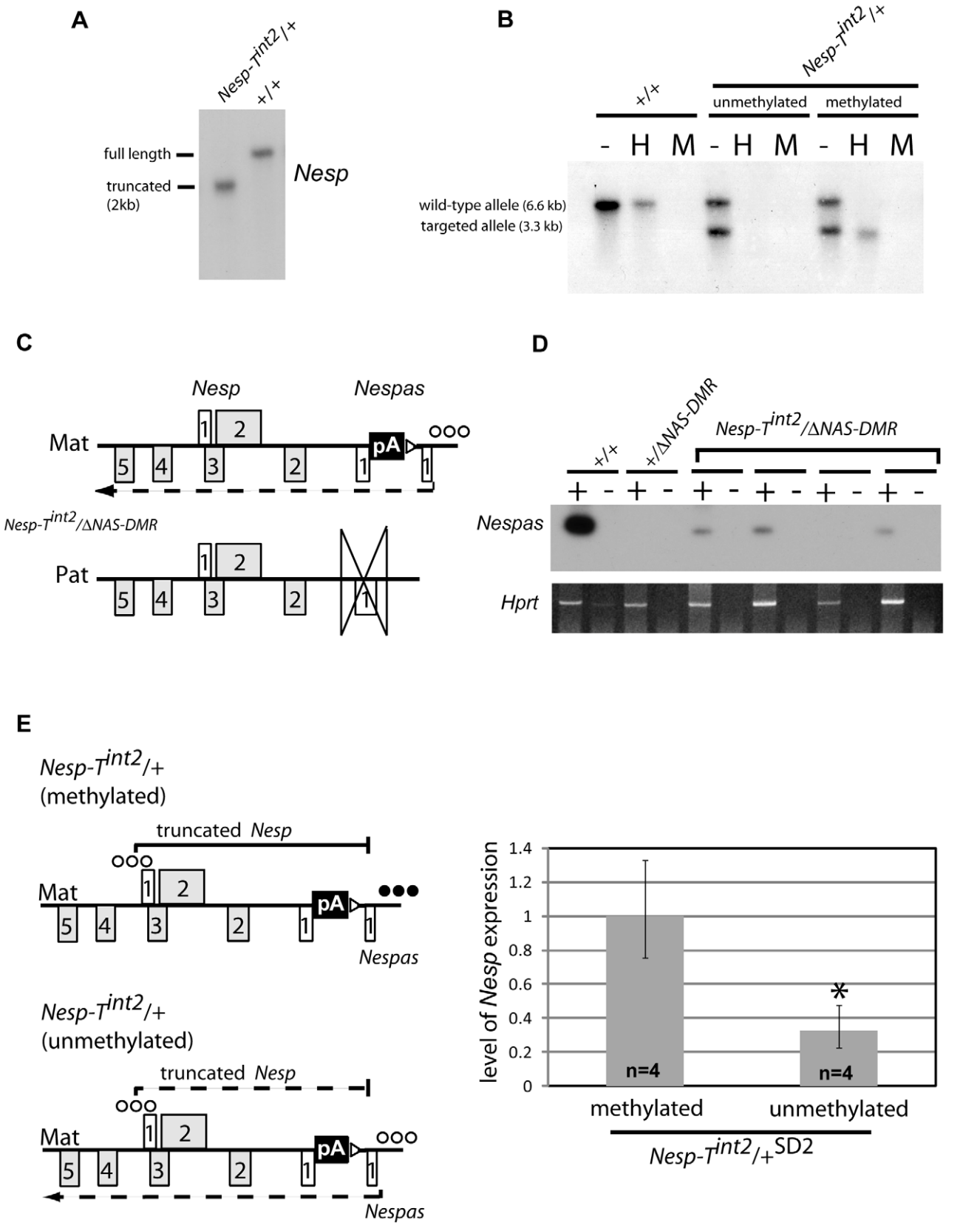

Figure 5. Maternal transmission of *Nesp-T*^{int2} results in downregulation of *Nesp* when the *Nespas* DMR is unmethylated. (A) The maternal *Nesp* transcript is truncated in *Nesp-T*^{int2}/+. RNA blot analysis showing expression of *Nesp* in poly(A)$^{+}$ RNA from 15.5 dpc embryos using the single stranded RNA probe shown in Figure 2C. (B) Southern analysis showing the *Nespas-Gnasxl* DMR promoter can be unmethylated or methylated on the maternal allele in *Nesp-T*^{int2}/+. Genomic DNA from newborn brain was digested with *Eco*RI (-), *Eco*RI and *Hpa*II (H), or *Eco*RI and *Msp*I (M) and

probed as shown in Figure S1. (C) Schematic showing the genomic organization of the double heterozygote with *Nesp-T*^{int2} maternally inherited and Δ*NAS-DMR* paternally inherited. The polyadenylation cassette, pA, truncates *Nesp* on the maternal allele and the ICR is deleted on the paternal allele. (D) RT-PCR showing *Nespas* is weakly expressed in neonatal brain from the maternally-derived targeted allele when the *Nespas* DMR is unmethylated. Primers were as described in Figure 2C. + and −, presence and absence of reverse transcriptase, respectively; *Hprt*, amplification control. (E, Left) Schematic summary of the transcriptional and methylation status of the maternal allele of *Nesp* and *Nespas* in *Nesp-T*^{int2}/+ (methylated) and *Nesp-T*^{int2}/+ (unmethylated) newborn brain. The polyadenylation cassette, pA truncates *Nesp* on the maternal allele. Row of filled circles, methylated allele; row of open circles, unmethylated allele. (E Right) Bar chart showing the relative level of *Nesp* expression in newborn brain by RT-qPCR between *Nesp-T*^{int2}/+^{SD2} littermates that had the *Nespas* DMR methylated and unmethylated. *Nesp* levels were measured using the TaqMan assay detecting exon 1 spliced onto exon 2. The level of *Nesp* was significantly lower in littermates that had the *Nespas* DMR unmethylated compared with those that had a methylated DMR ($P = 5.4\times10^{-3}$).
doi:10.1371/journal.pgen.1001347.g005

paternally expressed non-coding RNAs, *Aim* and *Kcnq1ot1* that are required for imprinted expression in *cis*. *Nespas* does have some similarities to both *Aim* and *Kcnq1ot1* in that it is necessary for imprinted expression, it is transcribed from a promoter contained within the unmethylated ICR on the paternal allele and has an antisense orientation with respect to the coding gene. *Tsix* appears

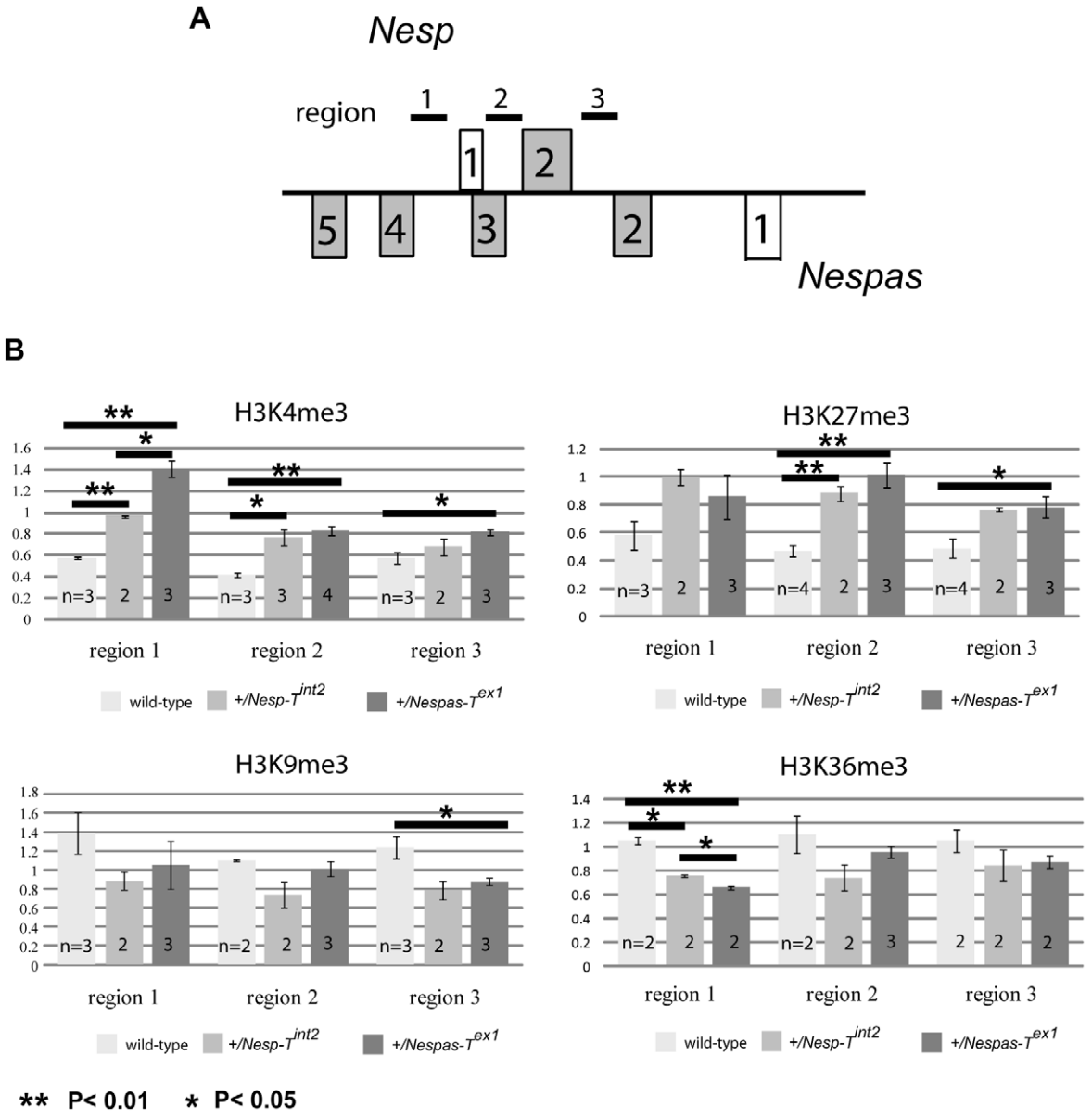

Figure 6. Paternal-specific histone modifications at *Nesp* in MEFs from wild-type, +/*Nesp-T*^{int2}, and +/*Nespas-T*^{ex1}. (A) Schematic showing the relative position of regions 1–3, amplified in the ChIP experiments at the 5′end of *Nesp*. (B) Bar chart showing the ratio of the bound paternal versus bound maternal band intensity for each chromatin modification. Each sample was normalised with the input, mock bound and mock unbound intensities. The ''n'' number on each bar chart represents the number of MEF lines analysed.
doi:10.1371/journal.pgen.1001347.g006

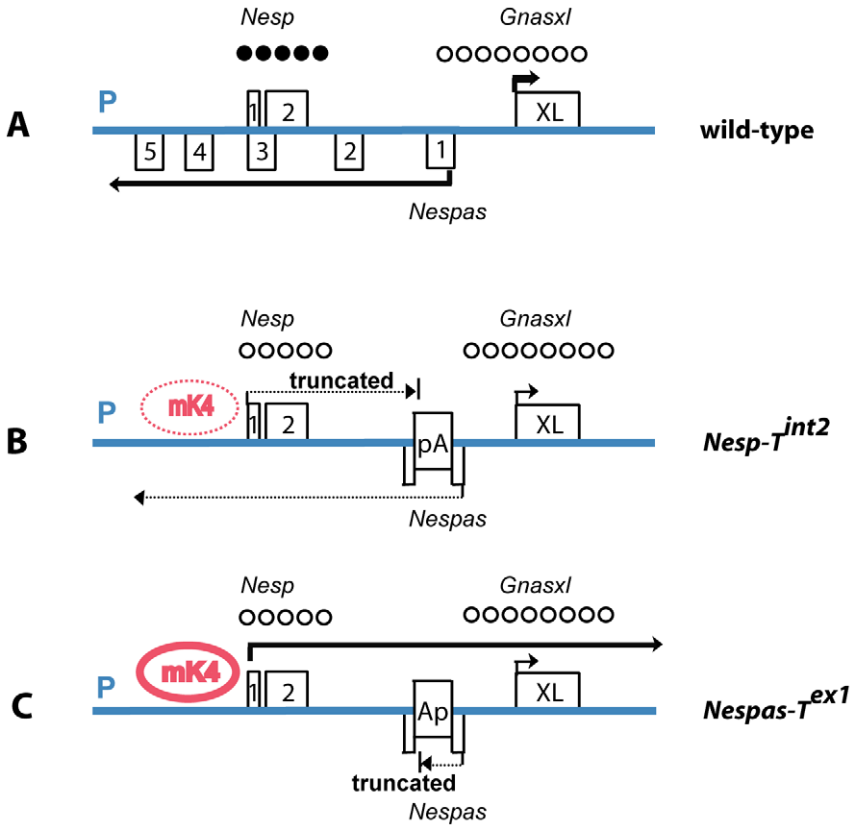

Figure 7. Summary of the transcriptional, methylation, and chromatin status of the paternal allele from *Nesp* to *Gnasxl* in wild-type and mutant mice. (A) wild-type; (B) +/*Nesp-T*^{int2} and (C) +/*Nespas-T*^{ex1}. The H3K4me3 mark, designated mK4 (in red) at the *Nesp* promoter is shown; bold text and circle, full enrichment of H3K4me3; normal text and dotted circle, partial enrichment of H3K4me3. Full length transcription of *Nesp* is shown in (C). The pA insertion truncates *Nesp* and the Ap insertion truncates *Nespas*. A low level of *Nespas* is sufficient to downregulate truncated *Nesp* levels in the absence of DNA methylation and this is associated with a reduction in the level of H3K4me3 at the *Nesp* promoter. The figure is not to scale.
doi:10.1371/journal.pgen.1001347.g007

to silence a single regulatory RNA whereas *Airn* and *Kcnq1ot1* silence multiple protein-coding genes in *cis*. There is evidence to suggest that *Airn* and *Kcnq1ot1* accumulate at some non-overlapping genes, in placenta, to mediate repressive histone modifications such as H3K9me3 and/or H3K27me3 in a manner similar to the silencing properties of *Xist* [30]. We have shown that *Nespas* regulates its sense counterpart *Nesp* but we do not yet have definitive evidence to show whether or not *Nespas* regulates other genes in the *Gnas* cluster.

Relationships among the levels of an antisense *Nespas*, its sense counterpart *Nesp*, and epigenetic marks

An inverse relationship exists on the paternal allele between the level of the non-coding RNA *Nespas* and the level of enrichment of the activating mark H3K4me3 associated with *Nesp* expression (summarised in Figure 7). As the level of the activating mark was different between the two insertion mutants +/*Nesp-T*^{int2} and +/*Nespas-T*^{ex1}, it was unlikely that the site of insertion of the cassette had disrupted a genomic sequence element controlling H3K4me3. We therefore conclude that the level of expression of the antisense *Nespas* modulates the level of H3K4me3 at the *Nesp* promoter, thereby modulating expression of *Nesp*. Our findings have parallels with the observation that silencing the tumour suppressor gene *p15* is modulated by its antisense RNA and expression of the antisense is also associated with a decrease in methylated H3K4 at the *p15* promoter [31].

We also identified a striking association between presence of H3K4me3 at the *Nesp* promoter in both mutants +/*Nesp-T*^{int2} and +/*Nespas-T*^{ex1}, and the absence of somatic DNA methylation. This was consistent with *in vitro* evidence that H3K4 methylation stops the acquisition of DNA methylation by preventing DNMT3L and DNMT3A from interacting with histone H3 [17,20]. Similar associations between chromatin and DNA methylation have been found at germline DMRs in somatic cells: chromatin on the DNA methylated alleles was devoid of H3K4 methylation whereas chromatin on the parental alleles without DNA methylation had high levels of H3K4 methylation [32,33]. We also noted a direct correlation between *Nespas* levels (or transcription) and the enrichment of H3K36me3 on the paternal allele. This alteration may also be relevant, since it has been shown recently that the PWWP domain of DNMT3A specifically recognises H3K36 trimethylation [21]. We presume the level of *Nespas* transcript or transcription was not high enough in the hypomorph to bring about and/or maintain DNA methylation at the *Nesp* promoter. This is consistent with the finding in an ES cell model where low levels of *Airn* transcription were associated with a lack of DNA methylation on the paternal *Igf2r* promoter [34].

Our chromatin analysis showed that demethylation of H3K4 rather than DNA methylation is a prerequisite for silencing *Nesp* on the paternal allele in the embryo. We propose the DNA methylation of *Nesp* that occurs post fertilisation is required to stabilise silencing long term. Silencing in the absence of DNA

methylation has previously been observed in placenta where imprinted genes in the *Kcnq1* cluster on distal chromosome 7 were silenced by repressive histone methylation [35]. The repressive histone marks were not completely effective at silencing the genes and it was suggested that this did not matter as the placenta is a short-lived organ. Evidence has been reported that DNA methylation at two somatic DMRs within the cluster is maintained by interaction of the non-coding *Kcnq1ot1* RNA with DNMT1 [36].

Model for how the level of an activating mark is controlled at the *Nesp* promoter

Prior to the *de novo* methylation of the *Nesp* DMR post fertilisation [10], we predict the *Nesp* promoter is enriched for H3K4 methylation. Consistent with this idea, H3K4me3 is present at the 5′ end of *Nesp* in mouse ES cells [25] and it has recently been shown that most zebrafish genes become marked by H3K4me3 when the genome is activated at the maternal to zygotic transition following fertilisation [37]. We propose that *Nespas* is required to remove the H3K4me3 mark at *Nesp* by recruiting histone demethylase(s) to the *Nesp* promoter region either by a transcript or transcription mediated mechanism. The demethylase(s) are needed to demethylate H3K4 to allow the somatic DMR to be methylated. A histone H3K4 demethylase (KDM1B) has been shown to be required for the establishment of some methylation imprints during oogenesis [38] but it is not known if a non-coding RNA is involved. KDM1B-deficient oocytes showed an increase in H3K4 methylation and failed to acquire DNA methylation marks at several ICRs. The recruitment of histone modifying enzymes by non-coding RNAs could be a common mechanism. There is evidence that in the placenta, *Airn* recruits G9A (KMT1C), a histone H3K9-methyltransferase to silence *Slc22a3* [39]. In addition, *Nespas* transcription may cause deposition of H3K36me3 across the *Nesp* promoter region such that, in combination, the two permissive histone marks provide a potent signal for the *de novo* methylation complex.

Alternatively the reduction in the activating mark H3K4me3 may be the consequence of the down-regulation of *Nesp* by *Nespas* by either a transcript or a transcription based mechanism. Given the complementarity between *Nesp* and *Nespas* RNAs, *Nesp* levels could be reduced by an RNA interference mechanism as reported for silencing *Xist* by *Tsix* [40]. Alternatively a transcription based model can be envisaged [41]. Thus a *cis*-acting element may lie within the *Nespas* transcription unit to silence *Nesp* completely. In the hypomorph the element will only be partially active so that transcription of *Nesp* can occur.

A second truncation allele of *Nesp*; truncation of *Nesp* in the second intron causes loss of germline methylation

As the transcription units of *Nesp* and *Nespas* overlap, the insertion of a polyadenylation cassette to generate the *Nesp-T^{int2}* allele not only created a *Nespas* hypomorph on the antisense strand but also created a truncated allele of *Nesp*, in intron 2, on the sense strand. A truncated allele *Nesp^{trun}*, had previously been generated at *Nesp* exon 2 [13]. In *Nesp-T^{int2}*/+, as previously observed with *Nesp^{trun}*/+, we also found loss of methylation at both the *Nespas-Gnasxl* and *Exon1A* DMRs. In addition we analysed a control, *Nespas-T^{ex1}*/+, whereby the cassette was inserted at the same site but in the opposite orientation. On the maternal allele, *Nesp* was fully expressed and the two DMRs remained methylated thus showing that the position of the insertion had not disrupted a DNA element that might be required for directing germline methylation. Thus the results from the second truncation allele are consistent with the proposal by Chotalia et al. [13] that transcription of *Nesp* across the DMRs in oocytes is required for the establishment of germline methylation marks within the *Gnas* cluster. Interestingly, with both truncation alleles, loss of methylation was detected at the *Nespas-Gnasxl* DMR in some mice but not others whereas the *Exon1A* DMR was invariably unmethylated. This occurred even though, in *Nesp-T^{int2}*/+, the truncated product of *Nesp* was longer than in *Nesp^{trun}*/+, and truncated at the start of the *Nespas-Gnasxl* DMR, much closer to the *Nespas-Gnasxl* DMR than in *Nesp^{trun}*. The variation in methylation at the *Nespas-Gnasxl* DMR may be due, at least in part, to variation in termination of *Nesp* transcription in the oocyte. Thus when the *Nespas-Gnasxl* DMR in *Nesp-T^{int2}*/+ is unmethylated, transcription termination must occur close to the polyadenylation site, but when the DMR is methylated there may be ineffective transcription termination. In support of this, full ablation of *Nesp* transcription by deletion of the *Nesp* DMR on the maternal allele caused almost complete loss of maternal methylation imprints [42].

Both maternal and paternal inheritance of *Nesp-T^{int2}* can result in similar epigenetic and transcriptional outcomes at *Nesp* and *Nespas*. Thus with paternal *Nesp-T^{int2}* and also with maternal *Nesp-T^{int2}* (in some animals) both the *Nesp* and *Nespas-Gnasxl* DMRs are unmethylated and *Nesp* and *Nespas* are weakly expressed, so that parental identity defining the imprinting of the wild-type allele has been lost. Although both maternal and paternal *Nesp-T^{int2}* can lead to similar epigenetic and transcriptional consequences the initiating events on the maternal and paternal alleles are probably different. On the maternal allele the primary event is likely to be the failure of *Nesp* transcription to induce methylation of the *Nespas-Gnasxl* DMR whereas on the paternal allele the primary event may be the failure of *Nespas* to methylate and fully suppress *Nesp*.

Materials and Methods

Targeting to generate *Nesp-T^{int2}* allele

The *Nesp-T^{int2}* targeting construct was designed to insert a polyadenylation cassette from the rabbit β-globin gene [5] into exon 1 of *Nespas*, in an orientation (designated pA) that would be expected to truncate *Nesp* (Figure 2A; between nucleotides 151519 and 151520, AL593857.10). The construct was generated by homologous recombination in yeast [43]. Briefly, a 1.2 kb fragment (nucleotides 31392-32553; M18818) from the rabbit β-globin gene, containing part of exon 2, complete intron 2 and exon 3 harbouring the polyadenylation signal was cloned into a *Xho*I site, 5′ of the *loxP* site flanking the selection cassette, in pRAY-Cre (AJ627603). The 5′ and 3′ recombinogenic arms (385 bp and 489 bp, respectively), extending upstream and downstream of the site of insertion of the polyadenylation cassette, were amplified by PCR; the 5′ arm was cloned 5′ of the polyadenylation cassette and the 3′ arm was cloned downstream of the 3′ *loxP* site. All primer sequences are available on request. A 10.9 kb mouse genomic *Spe*I-*Swa*I fragment, cloned in the yeast–*E. coli* shuttle vector pRS414 [8,44] was cotransformed into yeast YPH501 with a linear fragment comprising the recombinogenic arms, polyadenylation cassette and selection cassette using the yeast transformation kit (Sigma). The recombined shuttle vector was recovered from yeast colonies and used as the targeting vector (Figure 2A). The targeting vector was linearised with *Xba*I and electroporated into CJ7 mouse ES cells. Colonies surviving G418 selection were screened for correct targeting (pA-*neo* allele) by Southern analysis (Figure 2B). Genomic DNA from the clones was digested with *Nde*I and a 3′ external probe (nucleotides 157431-158817, AL593857.10) detected an 11.7 kb fragment in wild-type cells

and an 8.5 kb fragment in correctly targeted cells. Correct targeting at the 5′ end was confirmed by probing *Avr*II digested DNA with a 5′ external probe (nucleotides 144525-145690, AL593857.10; Figure 2B). The probe detected a 16.3 kb fragment in wild-type cells and a 12.9 kb fragment in correctly targeted cells. Two independently targeted clones, with no obvious chromosomal changes checked by karyotype analysis (E.P. Evans, personal communication), were injected into C57BL/6 × DBA/2 F2 blastocysts. Excision of the selection cassette occurred in the germline of male chimeras by testes-specific expression of Cre recombinase [45]. Proper excision of the cassette was confirmed by PCR amplification across the remaining *loxP* site (data not shown).

Targeting to generate *Nespas-T^{ex1}* allele

The *Nespas-T^{ex1}* construct was designed to insert the polyadenylation cassette, as described above, in the same site but in the reverse orientation to truncate *Nespas*. The targeting vector was made as described above except that the polyadenylation cassette was cloned in the opposite orientation in pRAY-Cre (Ap; Figure 4A). Southern blot analysis was performed, as described above, to identify correctly targeted cells (Ap-*neo* allele; Figure 4B). Two independently targeted clones were injected into C57BL/6J blastocysts.

Mouse breeding

Mice carrying the *Nesp-T^{int2}* and *Nespas-T^{ex1}* alleles were maintained on a 129/SvEv background. As +/*Nespas-T^{ex1}* mice were postnatal lethal, a breeding line had to be established by performing neonatal ovarian transfers as reported previously [8]. Offspring were genotyped for the *Nesp-T^{int2}* and *Nespas-T^{ex1}* alleles by PCR analysis of DNA from tail tips using a forward primer specific for the *loxP* region (5′-AGTACCCCGGGTTCGAAATC-3′) and a reverse primer specific to the arm (5′-CAAAATGGC-GAAACGGTTTG-3′). For some experiments, offspring of reciprocal crosses between *Nesp-T^{int2}*/+ or *Nespas-T^{ex1}*/+ and SD2 mice were produced. SD2 is a stock containing the distal portion of chromosome 2 from *Mus spretus* in a *Mus musculus* background [11]. Compound heterozygous *Nesp-T^{int2}*/Δ*NAS-DMR* mice were generated by crossing *Nesp-T^{int2}*/+ females with Δ*NAS-DMR*/+ males and offspring were genotyped for *Nesp-T^{int2}* and Δ*NAS-DMR* [8]. All mouse studies were done under the guidance issued by the Medical Research Council in "Responsibility in the Use of Animals for Medical Research" (July 1993) and under the authority of Home Office Project Licence Numbers 30/1518, 30/2526 and 30/1704.

Northern and RT-PCR analysis

Total RNA for RT-PCR was extracted from newborn brain using RNA-Bee (AMS Biotechnology) and DNA contamination was removed by treating the RNA with DNaseI (Message Clean kit; BioGene Ltd). RT-PCR was performed by reverse transcribing RNA with M-MLV reverse transcriptase (Invitrogen) and oligo(dT)$_{15}$ primer (Promega). A spliced form of *Nespas* was analysed using primers F6 and R2 as described previously [23]. Poly (A)$^+$ RNA for blot analysis was extracted using a FastTrack kit (Invitrogen). Northerns were performed as described previously [8].

Reverse Transcription-Quantitative Real-Time PCR (RT-qPCR)

Frozen tissues were homogenised using a 230 V Ultra-Turrax T25 basic homogeniser. Total RNA, extracted using the Allprep kit (Qiagen), was reverse transcribed using the High Capacity cDNA Reverse Transcription kit (Applied Biosystems). To avoid amplification of contaminating genomic DNA, samples were treated with RQ1 RNase-free DNase (Qiagen). The FAM dye-labelled TaqMan MGB probe and unlabelled primer sets (Table S1) for *Nesp* exon1/exon2 (assay ID nesp0-N0), *Nespas* intron 4 (assay ID AI88XP8) and *Gapdh* (assay ID Mm99999915_gl) were purchased from Applied Biosystems and all amplified with equal efficiency, at 99%, as determined from the slope of calibration curves [46]. The qPCR was performed with TaqMan Fast Universal PCR Master Mix (Applied Biosystems) using the 7500 Fast Real-Time PCR machine. The concentrations of the oligos at 1 × concentration were 900 nM for each primer and 200 nM for the probe. The expression levels of *Nespas* and *Nesp*, normalised to the reference gene *Gapdh*, were determined using the comparative threshold cycle method as described previously [47].

Methylation analysis

Methylation-sensitive Southern blot analysis of the *Nespas-Gnasxl* and *Nesp* promoter region was performed by digesting genomic DNA with *Eco*RI in combination with *Hpa*II and *Msp*I [8]. For bisulphite sequence analysis, purified genomic DNA from newborn brain was treated and amplified as described previously [9]. The DNA was treated using the EpiTect Bisulfite Kit (Qiagen). The primer sequences used to amplify each region are available in Table S1.

Chromatin Immunoprecipitation (ChIP) and PCR-SSCP

MEFs, derived from 13.5 dpc embryos from crosses of SD2 homozygous females with *Nesp-T^{int2}* and *Nespas-T^{ex1}* carrier males, were used for ChIP analysis as described previously [48]. Briefly, cells were collected and washed with PBS, the nuclei were purified using a sucrose cushion and incubated with MNase in order to obtain fragments of 1 to 3 nucleosomes in length. Approximately 20 μg of chromatin was incubated with 5 μg of antibody overnight at 4°C. The DNA from the ChIP was amplified by PCR and the parental alleles were distinguished by restriction digest and acrylamide gel electrophoresis. For each amplified region, the relative intensities of the maternal and paternal bands were measured using AIDA image analysis software (v3.27) in the ChIP input, the unbound fraction and antibody-bound fraction. We used antisera directed against trimethylated H3-Lys4 (Active Motif), trimethylated H3-Lys9 (Upstate), trimethylated H3-Lys27 (Abcam) and trimethylated H3-Lys36 (Abcam). The primer sequences for regions 1–3 are available in Table S1.

Supporting Information

Figure S1 The *Nespas-Gnasxl* region is unmethylated on the targeted allele in +/*Nesp-T^{int2}*. (A) Genomic DNA from neonatal brain was digested with *Eco*RI (-), *Eco*RI and *Hpa*II (H), or *Eco*RI and *Msp*I (M). (B) Schematic showing the probe and location of the 6.6 kb and 3.3 kb *Eco*RI fragments in the wild-type and targeted alleles, respectively.
Found at: doi:10.1371/journal.pgen.1001347.s001 (0.71 MB TIF)

Figure S2 Schematic representation of the splice variants detected from the splicing of *Nesp* into the inserted β-globin sequence on the paternal allele in +/*Nesp-T^{int2}* in newborn brain. *Nesp* transcription starts at exon 1 and the splice variants were amplified using a *Nesp* exon 2-specific forward primer and a reverse primer specific to the polyadenylation cassette (arrowheads show the position of the primers). The inserted sequence contains part of exon 2, complete intron 2 and exon 3 harbouring the polyadenylation signal of the β-globin gene. Thick black line labelled AATAAA is

part of the β-globin gene. Exon a (nucleotides 6187-6282, AJ251761); exon b (nucleotides 12997, AJ251761 - 31410, M18818); exon c (nucleotides 12843, AJ251761 - 31410, M18818).
Found at: doi:10.1371/journal.pgen.1001347.s002 (0.21 MB TIF)

Figure S3 *Nespas* is expressed and truncated in +/*Nespas-T*^{ex1}. (A) Sequence of truncation product from 3′ RACE showing transcription had been terminated in Nespas exon 1 at the expected position. The product was amplified with primers BIBR and linker-poly(dT) (Table S1) and confirms *Nespas* is polyadenylated. The direction of *Nespas* transcription is shown by an arrow and the polyadenylation signal is boxed. The 5′ end of *Nespas* is shown in bold type and the inserted sequence as grey type. The vertical line shows where exon 2 and exon 3 of the inserted β-globin sequence splice together. (B) Schematic representation of the *Gnas* cluster showing a *Ban*II variant between an allele of 129 (+^{129}) and C57BL/6 (+^{C57}). Arrowheads show the position of the primers; sequences are available in Table S1. (C) The RT-PCR assay uses the *Ban*II variant to distinguish the maternal and paternal transcripts of Nesp. Digestion with *Ban*II gives products of 964 bp for transcripts derived from the C57BL/6 allele and 909 bp for transcripts derived from the 129 allele.
Found at: doi:10.1371/journal.pgen.1001347.s003 (0.66 MB TIF)

Figure S4 Bisulphite sequence profile of the maternal allele of the *Nespas* DMR in double heterozygotes that had a maternal copy of *Nesp-T*^{int2} and were also heterozygous for a paternal copy of the Nespas promoter deletion Δ*NAS-DMR*. (A) double heterozygote that expressed *Nespas*, (B) double heterozygote in which *Nespas* was not detected.
Found at: doi:10.1371/journal.pgen.1001347.s004 (0.07 MB TIF)

Figure S5 Bisulphite sequence profile of the *Nesp* DMR on the maternal allele showing no gain of DNA methylation in *Nesp-T*^{int2}/+ (unmethylated). A variant between 129 SvEv and SD2 (nucleotide 140755; AL593857.10) allowed maternal and paternal alleles to be distinguished. Each row of circles represented a clone derived from the maternal allele and each circle corresponded to a separate CpG (filled circles, methylated CpGs; open circles, nonmethylated CpGs). Each block of circles represented the data from an individual mouse.
Found at: doi:10.1371/journal.pgen.1001347.s005 (0.51 MB TIF)

Figure S6 *Gnasxl* expression is reduced in both +/*Nesp-T*^{int2} and +/*Nespas-T*^{ex1}. Northern blot analysis of *Gnasxl* in poly (A)$^+$ RNA (μg) from 15.5 dpc embryos. The level of *Gnasxl* in the two mutants is substantially reduced. In +/*Nesp-T*^{int2}, the polyA cassette will truncate the *Nesp* transcript if transcribed from the paternal allele, and in +/*Nespas-T*^{ex1}, the polyA cassette will truncate the *Nespas* transcript. *Gnasxl* transcript is not expressed in +^{M}/+^{M}, mice with maternal uniparental disomy for the distal chromosome 2 imprinting region.
Found at: doi:10.1371/journal.pgen.1001347.s006 (0.90 MB TIF)

Figure S7 Loss of methylation on the maternal allele at the *Exon1A* DMR in both *Nesp-T*^{int2}/+ (methylated) and (unmethylated) samples. In *Nesp-T*^{int2}/+ (methylated), the *Nespas* DMR is methylated on the maternal allele whereas in *Nesp-T*^{int2}/+ (unmethylated), the *Nespas* DMR is unmethylated on the maternal allele. Genomic DNA from newborn lung was digested with *Bam*HI (-), *Bam*HI, and *Hpa*II (H), and *Bam*HI and *Msp*I (M). The probe was a 1.9 kb *Bam*HI - *Bgl*II fragment that encompasses exon 1A.
Found at: doi:10.1371/journal.pgen.1001347.s007 (0.56 MB TIF)

Figure S8 Bisulphite analysis showing the *Gnasxl* promoter region is unmethylated on the paternal allele in +/*Nespas-T*^{ex1}. A variant between 129 SvEv and SD2 (nucleotide 153610; AL593857.10) allowed maternal and paternal alleles to be distinguished. Each row of circles represents a clone derived from the paternal allele and each circle corresponds to a separate CpG (filled circles, methylated CpGs; open circles, nonmethylated CpGs). Each block of circles represents the data from an individual mouse.
Found at: doi:10.1371/journal.pgen.1001347.s008 (0.63 MB TIF)

Figure S9 Maternal inheritance of *Nespas-T*^{ex1} does not alter the imprinted expression of (B) *Nesp*, (C) *Gnasxl*, (D) *Exon1A*. Expression was analysed by RT-PCR in neonates using brain. (A) Schematic representation of the *Gnas* cluster showing a *Bst*UI variant between an allele of *M. spretus origin* (+^{SD2}) and an allele of *M. musculus origin* (+^{129}) to distinguish the maternal and paternal overlapping transcripts. Arrowheads show the position of the forward primers specific for each imprinted sense transcript and a common reverse primer in exon 12 of the *Gnas* gene (Williamson et al. [8]). The primer sequences are available in Table S1. RT-PCR products, shown in (B), (C) and (D) were digested with BstUI (Bst), which cuts at sites in the common set of downstream exons 2-12. Products of the same size but arising from alternative first exons, were detected. The additional site (Bst*) in the *M. spretus* derived allele but not the *M. musculus* allele allowed the maternal and paternal products to be distinguished. Neonates arising from reciprocal crosses between SD2 mice, which have a *M. musculus* genetic background but the distal region of chromosome 2 derived from *M. spretus* (+^{SD2}/+^{SD2}), and *M. musculus* carriers of *Nespas-T*^{ex1} were used.
Found at: doi:10.1371/journal.pgen.1001347.s009 (0.62 MB TIF)

Figure S10 The *Nespas-Gnasxl* DMR and the *Exon1A* DMR remain methylated when the *Nespas-T*^{ex1} is maternally inherited. (A) Differential methylation at the *Nespas-Gnasxl* promoter region. Genomic DNA was digested with *Eco*RI (-), *Eco*RI, and *Hpa*II (H), or *Eco*RI and *Msp*I (M). The *Nespas-Gnasxl* promoter region remained methylated on the targeted allele when the *Nespas-T*^{ex1} allele was maternally inherited. The probe is shown in Figure S1. (B) Methylation analysis at the *Exon1A* DMR. Wild-type (+/+) and *Nespas-T*^{ex1}/+ offspring, with a paternally derived *Exon1A* DMR deletion (+/Δ*Ex1A-DMR*, Williamson et al. [11]) were used to enable the methylation status of the maternal *Exon1A* DMR to be analysed in the absence of the paternal *Exon1A* DMR. Newborn brain genomic DNA was digested with *Bam*HI (-), *Bam*HI, and *Hpa*II (H), or *Bam*HI and *Msp*I (M) and probed with a 1.9 kb *Bam*HI - *Bgl*II fragment that encompasses exon 1A.
Found at: doi:10.1371/journal.pgen.1001347.s010 (0.57 MB TIF)

Table S1 Primer information.
Found at: doi:10.1371/journal.pgen.1001347.s011 (0.06 MB DOC)

Acknowledgments

We thank Denise Barlow and Frank Sleutels for kindly providing a cloned fragment from the rabbit β-globin gene. We also thank Nicola Powles-Glover for advice on MEF cell culture; the Mary Lyon Centre (MLC) Transgenics Service; staff of the MLC for animal husbandry, in particular Diane Napper, Lynn Jones, Jackie Harrison, and Sara Wells; and Steve Thomas and Kevin Glover for help with imaging.

Author Contributions

Conceived and designed the experiments: CMW GK JP. Performed the experiments: CMW STB CD SM CVB. Analyzed the data: CMW STB CD SM GK JP. Contributed reagents/materials/analysis tools: MF LT TND. Wrote the paper: CMW GK JP.

References

1. Mattick JS (2009) The genetic signatures of noncoding RNAs. PLoS Genet 5: e1000459. doi:10.1371/journal.pgen.1000459.
2. Williamson CM, Blake A, Thomas S, Beechey CV, Hancock J, et al. (2010) MRC Harwell, Oxfordshire. World Wide Web Site - Mouse Imprinting Data and References - http://www.har.mrc.ac.uk/research/genomic_imprinting/.
3. Edwards CA, Ferguson-Smith AC (2007) Mechanisms regulating imprinted genes in clusters. Curr Opin Cell Biol 19: 281–289.
4. Peters J, Robson JE (2008) Imprinted noncoding RNAs. Mamm Genome 19: 493–502.
5. Sleutels F, Zwart R, Barlow DP (2002) The non-coding Air RNA is required for silencing autosomal imprinted genes. Nature 415: 810–813.
6. Mancini-Dinardo D, Steele SJ, Levorse JM, Ingram RS, Tilghman SM (2006) Elongation of the Kcnq1ot1 transcript is required for genomic imprinting of neighboring genes. Genes Dev 20: 1268–1282.
7. Shin JY, Fitzpatrick GV, Higgins MJ (2008) Two distinct mechanisms of silencing by the KvDMR1 imprinting control region. EMBO J 27: 168–178.
8. Williamson CM, Turner MD, Ball ST, Nottingham WT, Glenister P, et al. (2006) Identification of an imprinting control region affecting the expression of all transcripts in the Gnas cluster. Nat Genet 38: 350–355.
9. Coombes C, Arnaud P, Gordon E, Dean W, Coar EA, et al. (2003) Epigenetic properties and identification of an imprint mark in the Nesp-Gnasxl domain of the mouse Gnas imprinted locus. Mol Cell Biol 23: 5475–5488.
10. Liu J, Yu S, Litman D, Chen W, Weinstein LS (2000) Identification of a methylation imprint mark within the mouse Gnas locus. Mol Cell Biol 20: 5808–5817.
11. Williamson CM, Ball ST, Nottingham WT, Skinner JA, Plagge A, et al. (2004) A cis-acting control region is required exclusively for the tissue-specific imprinting of Gnas. Nat Genet 36: 894–899.
12. Liu J, Chen M, Deng C, Bourc'his D, Nealon JG, et al. (2005) Identification of the control region for tissue-specific imprinting of the stimulatory G protein alpha-subunit. Proc Natl Acad Sci U S A 102: 5513–5518.
13. Chotalia M, Smallwood SA, Ruf N, Dawson C, Lucifero D, et al. (2009) Transcription is required for establishment of germline methylation marks at imprinted genes. Genes Dev 23: 105–117.
14. Bourc'his D, Xu GL, Lin CS, Bollman B, Bestor TH (2001) Dnmt3L and the establishment of maternal genomic imprints. Science 294: 2536–2539.
15. Hata K, Okano M, Lei H, Li E (2002) Dnmt3L cooperates with the Dnmt3 family of de novo DNA methyltransferases to establish maternal imprints in mice. Development 129: 1983–1993.
16. Kaneda M, Okano M, Hata K, Sado T, Tsujimoto N, et al. (2004) Essential role for de novo DNA methyltransferase Dnmt3a in paternal and maternal imprinting. Nature 429: 900–903.
17. Ooi SK, Qiu C, Bernstein E, Li K, Jia D, et al. (2007) DNMT3L connects unmethylated lysine 4 of histone H3 to de novo methylation of DNA. Nature 448: 714–717.
18. Jia D, Jurkowska RZ, Zhang X, Jeltsch A, Cheng X (2007) Structure of Dnmt3a bound to Dnmt3L suggests a model for de novo DNA methylation. Nature 449: 248–251.
19. Jurkowska RZ, Anspach N, Urbanke C, Jia D, Reinhardt R, et al. (2008) Formation of nucleoprotein filaments by mammalian DNA methyltransferase Dnmt3a in complex with regulator Dnmt3L. Nucleic Acids Res 36: 6656–6663.
20. Zhang Y, Jurkowska R, Soeroes S, Rajavelu A, Dhayalan A, et al. (2010) Chromatin methylation activity of Dnmt3a and Dnmt3a/3L is guided by interaction of the ADD domain with the histone H3 tail. Nucleic Acids Res 38: 4246–4253.
21. Dhayalan A, Rajavelu A, Rathert P, Tamas R, Jurkowska RZ, et al. (2010) The Dnmt3a PWWP domain reads histone 3 lysine 36 trimethylation and guides DNA methylation. J Biol Chem 285: 26114–26120.
22. Wroe SF, Kelsey G, Skinner JA, Bodle D, Ball ST, et al. (2000) An imprinted transcript, antisense to Nesp, adds complexity to the cluster of imprinted genes at the mouse Gnas locus. Proc Natl Acad Sci U S A 97: 3342–3346.
23. Williamson CM, Skinner JA, Kelsey G, Peters J (2002) Alternative non-coding splice variants of Nespas, an imprinted gene antisense to Nesp in the Gnas imprinting cluster. Mamm Genome 13: 74–79.
24. Li T, Vu TH, Ulaner GA, Yang Y, Hu JF, et al. (2004) Activating and silencing histone modifications form independent allelic switch regions in the imprinted Gnas gene. Hum Mol Genet 13: 741–750.
25. Mikkelsen TS, Ku M, Jaffe DB, Issac B, Lieberman E, et al. (2007) Genome-wide maps of chromatin state in pluripotent and lineage-committed cells. Nature 448: 553–560.
26. Kolasinska-Zwierz P, Down T, Latorre I, Liu T, Liu XS, et al. (2009) Differential chromatin marking of introns and expressed exons by H3K36me3. Nat Genet 41: 376–381.
27. Lindroth AM, Park YJ, McLean CM, Dokshin GA, Persson JM, et al. (2008) Antagonism between DNA and H3K27 methylation at the imprinted Rasgrf1 locus. PLoS Genet 4: e1000145. doi:10.1371/journal.pgen.1000145.
28. Rougeulle C, Avner P (2004) The role of antisense transcription in the regulation of X-inactivation. Curr Top Dev Biol 63: 61–89.
29. Penny GD, Kay GF, Sheardown SA, Rastan S, Brockdorff N (1996) Requirement for Xist in X chromosome inactivation. Nature 379: 131–137.
30. Nagano T, Fraser P (2009) Emerging similarities in epigenetic gene silencing by long noncoding RNAs. Mamm Genome 20: 557–562.
31. Yu W, Gius D, Onyango P, Muldoon-Jacobs K, Karp J, et al. (2008) Epigenetic silencing of tumour suppressor gene p15 by its antisense RNA. Nature 451: 202–206.
32. Delaval K, Govin J, Cerqueira F, Rousseaux S, Khochbin S, et al. (2007) Differential histone modifications mark mouse imprinting control regions during spermatogenesis. EMBO J 26: 720–729.
33. Kacem S, Feil R (2009) Chromatin mechanisms in genomic imprinting. Mamm Genome 20: 544–556.
34. Stricker SH, Steenpass L, Pauler FM, Santoro F, Latos PA, et al. (2008) Silencing and transcriptional properties of the imprinted Airn ncRNA are independent of the endogenous promoter. EMBO J 27: 3116–3128.
35. Lewis A, Mitsuya K, Umlauf D, Smith P, Dean W, et al. (2004) Imprinting on distal chromosome 7 in the placenta involves repressive histone methylation independent of DNA methylation. Nat Genet 36: 1291–1295.
36. Mohammad F, Mondal T, Guseva N, Pandey GK, Kanduri C Kcnq1ot1 noncoding RNA mediates transcriptional gene silencing by interacting with Dnmt1. Development 137: 2493–2499.
37. Vastenhouw NL, Zhang Y, Woods IG, Imam F, Regev A, et al. (2010) Chromatin signature of embryonic pluripotency is established during genome activation. Nature 464: 922–926.
38. Ciccone DN, Su H, Hevi S, Gay F, Lei H, et al. (2009) KDM1B is a histone H3K4 demethylase required to establish maternal genomic imprints. Nature 461: 415–418.
39. Nagano T, Mitchell JA, Sanz LA, Pauler FM, Ferguson-Smith AC, et al. (2008) The Air noncoding RNA epigenetically silences transcription by targeting G9a to chromatin. Science 322: 1717–1720.
40. Ogawa Y, Sun BK, Lee JT (2008) Intersection of the RNA interference and X-inactivation pathways. Science 320: 1336–1341.
41. Pauler FM, Koerner MV, Barlow DP (2007) Silencing by imprinted noncoding RNAs: is transcription the answer? Trends Genet 23: 284–292.
42. Frohlich LF, Mrakovcic M, Steinborn R, Chung UI, Bastepe M, et al. (2010) Targeted deletion of the Nesp55 DMR defines another Gnas imprinting control region and provides a mouse model of autosomal dominant PHP-Ib. Proc Natl Acad Sci U S A 107: 9275–9280.
43. Storck T, Kruth U, Kolhekar R, Sprengel R, Seeburg PH (1996) Rapid construction in yeast of complex targeting vectors for gene manipulation in the mouse. Nucleic Acids Res 24: 4594–4596.
44. Plagge A, Gordon E, Dean W, Boiani R, Cinti S, et al. (2004) The imprinted signaling protein XL alpha s is required for postnatal adaptation to feeding. Nat Genet 36: 818–826.
45. Bunting M, Bernstein KE, Greer JM, Capecchi MR, Thomas KR (1999) Targeting genes for self-excision in the germ line. Genes Dev 13: 1524–1528.
46. Bustin SA, Benes V, Garson JA, Hellemans J, Huggett J, et al. (2009) The MIQE guidelines: minimum information for publication of quantitative real-time PCR experiments. Clin Chem 55: 611–622.
47. Lu C, Schwartzbauer G, Sperling MA, Devaskar SU, Thamotharan S, et al. (2001) Demonstration of direct effects of growth hormone on neonatal cardiomyocytes. J Biol Chem 276: 22892–22900.
48. Fournier C, Goto Y, Ballestar E, Delaval K, Hever AM, et al. (2002) Allele-specific histone lysine methylation marks regulatory regions at imprinted mouse genes. EMBO J 21: 6560–6570.
49. Peters J, Williamson CM (2007) Control of imprinting at the Gnas cluster. Epigenetics 2: 207–213.